© creative

Scientific paper

Theoretical Study of the Stabilization of Lysine Through Pseudocyclic Conformation

Germán Ávila-Sierra¹, Aned de Leon^{2,1,*}, Ramón Ochoa-Landín³, Santos Jesús Castillo¹, José Luis Cabellos⁴

¹ Departamento de Investigación en Física, Universidad de Sonora, Blvd. Luis Encinas y Rosales S/N Centro, Hermosillo, 8300, México

² Departamento de Ciencias Químico-Biológicas, Universidad de Sonora, Blvd. Luis Encinas y Rosales S/N Centro, Hermosillo, 8300, México

³ Departamento de Física, Universidad de Sonora, Blvd. Luis Encinas y Rosales S/N Centro, Hermosillo, 8300, México

⁴ Universidad Politécnica de Tapachula. Carretera a Puerto Madero km 24+300, San Benito, Puerto Madero C.P. 30830 Tapachula, Chiapas.

* Corresponding author: E-mail: author: aned.deleon@unison.mx

Received: 12-05-2024

Abstract

This study investigates lysine's conformational behavior and thermal properties at the PBE0-GD3/Def2-TZVP level for geometry optimizations and CCSD(T)/Def2-TZVP level of theory for the calculation of thermal population. Lysine forms pseudocyclic conformations stabilized by hydrogen bonds between amino and carboxyl groups. We identified 36 conformers, split evenly between L- and D-lysine, with small energy differences between structures. When the pseudocyclic conformation is disrupted, the energy is highly affected. Lysine's geometries are remarkably sensitive to temperature. These findings highlight lysine's temperature sensitivity and its potential for diverse applications. Its structural plasticity across 0–1800 K suggests roles in material science, such as temperature-responsive semiconductor thin films, coatings, sensors, catalysis through tunable active sites, and biomedicine for drug delivery or protein stabilization. The insights provided by this study emphasize lysine's versatility as a biomolecule and its implications for technological innovation across multiple fields.

Keywords: Lysine, enantiomers, temperature, pseudocycle, theoretical study

1. Introduction

L-Lysine portrays unique structural and nucleophilic characteristics. The lysine ε-amino group is the most nucleophilic after cysteine. This allows it to participate in the active sites of enzymes. Under physiological conditions the lysil chain is less nucleophilic. Anyhow, environmental effects can reduce the pKa thus increasing its reactivity. Its conformational distributions are highly affected not only by pKa, but also by solvents and temperature. Mirtič and Grdadolnik reported that the energy minima structures of poly-L-lysine (PLL) were highly dependent on solvents. In the presence of water, PLL shows an extended configuration, while ethanol and glycerol produce a more compact structure. This study found that the configuration

of PLL is stabilized through the competition between the formation of inter and intramolecular hydrogen bonds, which varies from solvent to solvent. As well as solvents, temperature plays an important role in its configuration. Studies show that temperature changes in proteins with lysine side chains cause them to modify their orientation and hydrogen bonding. These structural changes both in isolation and within proteins can have crucial implications for biological functions. 9,10

Most works are dedicated to study L-amino acids since they are more common in biological systems than D-enantiomers. Several studies for L-enantiomers have been dedicated to their understanding. For instance, Tulip et. al studied the structural and electronic properties of L-amino acids such as alanine, leucine, isoleucine

and valine using DFT.¹⁴ Bowden et al. analyzed the solubility in mixed solvents of L-amino acids.¹⁵ Lakhera et al. performed a theoretical study on the spectral and optical properties of essential L-amino acids such as histidine, isoleucine, leucine and lysine.¹⁶ Aliyeba et al. studied the electrolyte effects on the amino acid solubility.¹⁷ Liu et al. used DFT to investigate the interaction between zwitterionic amino acids and several metal cations in aqueous solutions.¹⁸ Barria-Urrenda et al. studied the adsorption of proteinogenic L-amino acids onto pristine graphene using free-energy calculations to understand the thermodynamic contributions and potential applications in protein-graphene interactions.¹⁹

Although L-amino acids are more likely found in nature, D-enantiomers are still present in various living organisms. Particularly, they have been found in their free form in the brain and nervous system, yet also in peptides, proteins,²⁰ bacterial cell walls²¹ and food sources.²² Specifically, D-lysine may play a part in neurotransmission and perhaps in the control of certain diseases^{22–26} such as amyotrophic lateral sclerosis (ALS),²³ schizophrenia²⁴ and cancer²⁷. Only few works are dedicated to theoretically study D-enantiomers. For instance, Poline et al. researched the infrared signatures of proton-bound homochiral and heterochiral dimers of five amino acids (serine, alanie, threonine, phenylalanine, and arginine).²⁸ Aliashkevich et al. review the biological roles of D-amino acids and how they influence bacterial physiology and biodiversity.²⁹ Xu et al. review the use of amino acids, including D-enantiomers for modifying the structure of natural products to enhance biological activity or stability.³⁰

Although there are theoretical studies on L-lysine, ^{31,32} none of them study both L- and D-lysine. Although Boeckx et al.³¹ performed a temperature-dependent conformational analysis, they did it at specific conditions. Besides, their study used DFT and MP2 which could be more accurate to describe the dispersion forces involved in these systems. Therefore, we propose the study of D- and L-enantiomers, exploring the temperature effects at a wide range of temperatures (0-600 K), a more accurate high-level computational approach (PBE0-GD3/Def2TZVP without and with PCM solvent (water) effects for geometry optimizations, thermal population calculations, and the introduction of the concept of pseudocyclic stabilization in lysine through hydrogen bonds. Single point calculations at the CCSD(T)/ Def2-TZVP level were performed to compare the energies with those at DFT level.

2. Theoretical Methods

2. 1. Computational Details

We employed the DFT ensemble procedure which is valid for finite temperatures³³ above 0K to emulate experimental conditions. To inspect the potential free energy surface, we utilized stochastic kick methodology imple-

mented in Bilatu software. 34,35 Optimizations were performed via ORCA software.36 Initial searches were at the PBE0/37Def2TZVP38 level together with the Grimme dispersion correction GD3³⁹ integrated with the conformational search code (CSC). 960 conformers were generated with random alteration of dihedral angles, as in other conformational search algorithms⁴⁰ in Python included in the global search of the GALGOSON code. 41,42 We confirmed that all structures are true minima through an analysis of their harmonic vibrational frequencies analysis. Secondly, we calculated single point calculations of energy minima systems at the domain based local pair natural orbital coupled cluster single, double and perturbative triples CCS-D(T)43,44/Def2-TZVP level of theory. Finally, we included solvent effects using the polarizable continuum model (PCM)⁴⁵ at the PBE0-GD3/Def2-TZVP level.

The thermochemistry properties were calculated based on references. $^{46-49}$ The Boltzmann populations were computed using a temperature-dependent statistical thermodynamics approach based on the molecular partition function. Importantly, the free energy values were not recomputed at each temperature via separate DFT calculations, but instead derived from a single set of vibrational frequency calculations performed at 0 K. These frequencies were then used to calculate temperature-dependent thermodynamic quantities—such as entropy and enthalpy—via standard statistical mechanical formulas (under harmonic oscillator and rigid rotor approximations). The Gibbs free energy at any given temperature was then computed from these quantities using G = H - TS and used to evaluate Boltzmann populations using the following equation:

$$P_i(T) = \frac{e^{-i\beta\Delta G^k}}{\sum e^{-i\beta\Delta G^k}} \tag{1}$$

Where is the Gibbs free energy difference of the *i-th* isomer with respect to the lowest energy structure, and $\beta = 1/k_B T$. The entropic contributions, including effects due to molecular symmetry, were included, as they can significantly affect relative populations at finite temperatures.

This approach is consistent with prior work on nanoclusters \$^{41,42,50}\$. It has yielded physically meaningful results across wide temperature ranges, and the vibrational contributions (which dominate at low to intermediate temperatures) remain reliable under the harmonic approximation up to about 600 K, which is the upper limit considered in this study.

3. Results and Discussion

3. 1. Energy Minima Structures

Through our stochastic search for local minima on the PES we obtained 30 conformations (See Table 1 and Figs. S1 and S2 in the Supplementary Material). Fig.S1 displays energy minima structures calculated with PBE0-GD3/Def2-TZVP. We obtained single point calculations for these same structures at the CCSD(T)/Def2-TZVP. Finally, Fig.S2 shows energy minima structures at the PBE0-GD3/Def2-TZVP level with the PCM with water as solvent. L- and D-enantiomers presented very similar energy values.

For the case of no solvent, Fig. S1 shows the energy minima geometries in order of increasing relative energy. Structures 1–9 all display a pseudo-cyclic structure caused by the formation of 2 hydrogen bonds. Structures 1, 3, 6 and 8 have a carboxyl group forming hydrogen bonds with the 2 amino groups. Geometries 2, 4, 5 and 7 form one hydrogen bond between the hydroxyl part of the carboxyl group and the terminal amino group, and a second one between the carbonyl part of the carboxyl group and the middle amino group. Up to structure 8, the relative energy is of 1.602 kcal/mol. Thus, the energy differences between these structures is small. Structure 9 has a higher energy difference, with a relative energy of 2.606 kcal/mol for D-lysine and 2.610 for L-lysine. Although structures 9 also form 2 hydrogen bonds, but one of them is formed differently than in the past structures. As in structures 1, 3, 6 and 8, one of the hydrogen bonds is formed between the amino groups. However, the other one is formed between the hydroxyl part of the carboxyl group and the terminal amino group, instead of the middle one as in aforementioned structures.

Starting from geometries 10, an important energy gap is observed, which is reflected in a loss of a hydrogen bond that breaks the main pseudo-cyclic configuration. The energy differences are of 6.000 kcal for L-lys and 6.304 kcal/mol for D-lys. From this point on, the terminal amino group no longer forms hydrogen bonds. The only hydrogen bond formed is between the middle amino group and the carboxyl group.

The single point energies at the CCSD(T)/Def2-TZ-VP level, denoted as ECCSD(T), exhibit a clear energetic trend that mirrors the stability observed in the DFT-optimized structures. Structures 1 through 8 for both L- and D-lysine remain within a narrow energy window (≤ 1.613 kcal/mol), highlighting the stabilizing effect of dual intramolecular hydrogen bonds characteristic of pseudocyclic conformations. Structure 9, while still forming two hydrogen bonds, shows a marked increase in energy (≈3.525 kcal/mol), suggesting a less optimal bonding geometry. A substantial energy gap is then observed starting from structure 10, with relative energies between 9.636 kcal/mol and 10.769 kcal/mol. This abrupt shift reflects the loss of the second stabilizing hydrogen bond-particularly the one involving the terminal amino group-leading to significant conformational destabilization. These results reinforce the crucial role of hydrogen bond topology in lysine's energetic landscape and validate the importance of high-level correlation methods like CCSD(T) for accurately assessing conformational hierarchies.

The PCM water effects modified the geometries slightly, as shown in Fig. S2. Simlarly to Fig. S1, we present only 30 structures (1'–15' for both L and D enantiomers). However, the effect on the energies was more noticeable (see Table 1). The highest relative energy for structures 1'–9' was of 3.176 kcal/mol. There remains an energy gap for structures 10'–18' compared to those of 1'–9'. The relative energies range from 9.283–11.900 kcal/mol. The pseudocyclic configuration remains. Yet, it can be noted than upon solvent effects, the most favored structures are those that form one hydrogen bond between the hydroxyl part of the carboxyl group and the terminal amino group, and a second one between the carbonyl part of the carboxyl group and the middle amino group. The only exception are

Table 1. Relative energies in kcal·mol $^{-1}$. E_{PBE0} stands for the relative energies with zero-point correction of optimized structures at the PBE0-GD3/Def2-TZVP level; $E_{CCSD(T)}$ represents the energies at the CCSD(T)/Def2-TZVP level and E_{PCM} , the energies using the PCM water effects at the PBE0-GD3/Def2-TZVP.

Structure	$\mathbf{E_{PBE0}}$		$E_{CCSD(T)}$		Structure	$\mathbf{E}_{\mathbf{PCM}}$	
	L	L	L	D		L	D
1	0	0	0.300	0.300	1'	0	0
2	0.314	0.314	0.000	0.000	2'	0.135	0.135
3	0.733	0.733	0.767	0.767	3'	0.993	0.993
4	1.023	1.023	1.613	1.613	4'	1.497	1.498
5	1.035	1.035	1.588	1.588	5'	1.584	1.584
6	1.042	1.042	1.407	1.407	6'	2.085	2.085
7	1.235	1.235	1.011	1.013	7'	2.497	2.497
8	1.602	1.602	1.345	1.345	8'	2.89	2.89
9	2.61	2.61	3.525	3.525	9'	3.176	3.176
10	8.911	8.911	10.486	10.486	10'	9.283	9.283
11	9.311	9.311	9.700	9.700	11'	9.786	9.786
12	9.577	9.577	9.636	9.636	12'	9.799	9.799
13	9.924	9.924	10.560	10.560	13'	10.364	10.364
14	9.948	9.948	10.273	10.273	14'	10.805	10.805
15	10.095	10.095	10.769	10.769	15'	11.095	11.095

structures 4', which shares a very similar configuration to structures 1. Following in energy are those structures that form one hydrogen bond between the amino groups and the other one between the middle amino group and the carboxyl group.

3. 2. Thermal Properties

ly, as we reported previously.⁴⁹ As temperature rises, the probability of structures 2-L and 2-D start to reduce while that of structures 1-L and 1-D increase.

At 188 K, structures 1 and 2 and their enantiomers are equiprobable. A similar behavior has been observed for arginine at 335K.⁴⁹ For the case of arginine, once the first two structures and their enantiomers become equiproba-

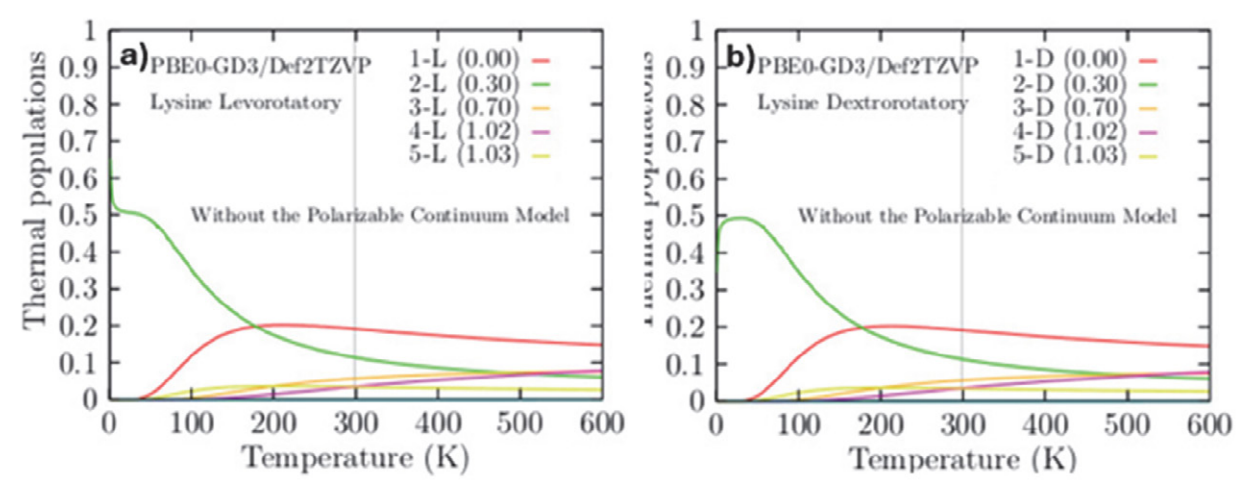


Fig. 1. Relative population for temperature 0-600 K at the PBE0-GD3/Def2TZVP level for a) L-lys and b) D-lys.

For simplicity, we selected the first 5 structures which have the lowest relative energy values to analyze the trend in relative population, as portrayed in Fig. 1. At temperatures below 188K, structures 2-L and 2-D are exponentially more probable than structure 1-L and 1-D. Although the geometry between structures 1 and 2 is only slightly different, at low temperatures the degrees of freedom of the molecules is the lowest. This implies that the interconversion of one geometry to the other has a low probability. At higher temperatures, kinetic energy elevates, allowing the interconversion of one geometry to another more like-

ble, they keep being so up until around 1100 K. Lysine, on the other hand, is more likely to be found as structure 2 below 188 K and above this temperature, switches to structure 1. In the relative population graph for Arg. (Fig. 3 in ref.⁴⁹) through the whole domain of temperatures, there is only 1 curve that crosses all of them. In contrast to Arg, in Lysine's relative population graph, multiple curves cross at different points. This shows a higher sensibility of Lysine's geometry towards temperature.

As shown in Fig. 2, upon solvent effects, structures 1'L and 1'D cross at around 400K with 2'L and 2'D. Any-

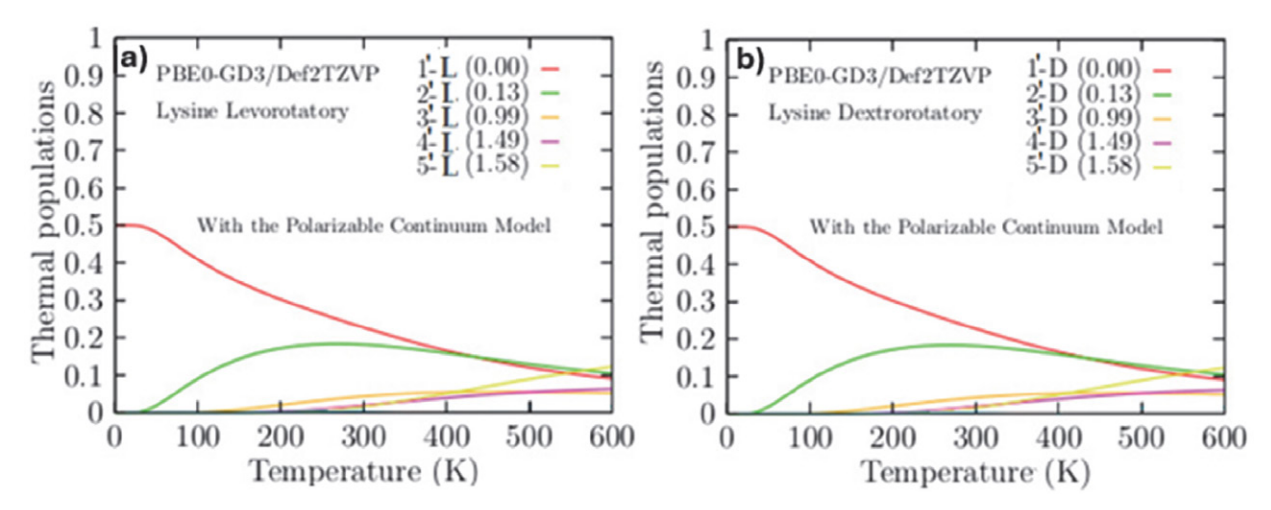


Fig. 2. Relative population for temperature 0-600 K at the PBE0-GD3/Def2TZVP level with PCM solvent effects for a) L-lys and b) D-lys.

how, they remain very similar in probability, in contrast to Fig.3, where the absence of solvent effects drives the two curves noticeably farther apart. The rest of the curves remain below those of 1 and 2, except for geometries 5'L and 5'D, which at around 381K become the highest in probability.

4. Conclusions

The main contributions for lysine's stability are 2 hydrogen bonds among the amino groups and the carboxyl group. This creates a pseudocyclic conformation. When the terminal amino group does not form a hydrogen bond, the main pseudocyclic structure is broken, which highly affects the stability. This is shown in the relative energy values in Table 1. This is true for both models: without solvent effects and with them. The main difference lies in a preference for certain interactions in the structures with the PCM water effects. It favors those structures that form a hydrogen bond between the hydroxyl part of the carboxyl group and the terminal amino group, and a second one between the carbonyl part of the carboxyl group and the middle amino group.

High-level single point calculations at the CCSD(T)/Def2-TZVP level confirmed the energetic trends predicted by DFT, emphasizing the critical role of dual intramolecular hydrogen bonds in stabilizing pseudocyclic conformations. The marked energy gap observed upon disruption of these interactions further underscores their relevance in determining the conformational hierarchy of lysine.

The geometries are also sensitive to temperature. Different geometries compete, which means that throughout the wide range of temperatures (0–600 K), lysine can be found as a mixture of structures. In the presence of water, this also happens. Yet, the temperature at which geometries interconvert is higher. Without solvent, they interconvert at around 188K, while under the effect of water, at 381K.

Lysine's structural adaptability across a wide temperature range presents opportunities in diverse fields. In material science, it could enable temperature-responsive semiconductor thin films, coatings, biosensors, or nanotechnologies. In catalysis, lysine's versatility may facilitate temperature-tunable or stabilizing roles in reactions. Pharmaceuticals and biotechnology could benefit from lysine-based smart drug delivery systems, protein stabilizers, or bioengineered polymers. It also holds promise in the food industry for temperature-sensitive nutrient release, in energy applications as high-temperature sensors or CO₂ capture materials, and in structural biology for studying protein folding and molecular interactions. These applications leverage lysine's resilience, biocompatibility, and dynamic structural properties, making it valuable in innovation across disciplines.

Acknowledgements

We thank CONACyT for its support. Also, we are grateful to the High-Performance Computing Area of the University of Sonora (ACARUS).

5. References

- S. M. Hacker, K. M. Backus, M. R. Lazear, S. Forli; B. E. Correia, B.F. Cravatt, *Nature Chem.* 2017, 9,1181–1190.
 DOI:10.1038/nchem.2826
- A. H. K. Al Temimi, H. I. V. Amatdjais-Groenen, Y. V. Reddy,
 R. H. Blaauw, H. Guo, P. Qian, J. Mecinović, *Commun. Chem.* 2019, 2, 112. DOI:10.1038/s42004-019-0210-8
- 3. H. Kondo, M. Kitagawa, Y. Matsumoto, M. Amano, S. Sugiyama, T. Tamura, H. Kusakabe, K. Inagaki, K. Imada, *Protein Sci.* **2020**, *29*, 2213–2225. **DOI**:10.1002/pro.3946
- V. D'Annibale, D. Fracassi, P. Marracino, G. D'Inzeo, M. D'Abramo, *Molecules* 2022, 27, 6454–6466.
 DOI:10.3390/molecules27196454
- A. Mirtič, J. Grdadolnik, *Biophys. Chem.* 2013, 175, 47–53.
 DOI:10.1016/j.bpc.2013.02.004
- R. Rousseau, E. Schreiner, A. Kohlmeyer, D. Marx, *Biophys. J.* 2004, 86, 1393–1407. DOI:10.1016/S0006-3495(04)74210-1
- C. C. Cornilescu, G. Cornilescu, H. Rao, S. F. Porter, M. Tonelli, M. L. DeRider, J. L. Markley, F. M. Asadi-Porter, *Proteins* 2014, 81, 919–925. DOI:10.1002/prot.24259
- H. Chen, J. Deng, Q. Cui, K. Henzler-Wildman, *Biophys. Comput. Biol.* 2021, 118, e2017280118.
 DOI:10.1073/pnas.2017280118
- L. Stagi, M. Sini, D. Carboni, R. Anneda, G. Siligardi, T. M. Gianga, R. Hussain, P. Innocenzi, Sci. Rep. 2022, 12, 19719–19731. DOI:10.1038/s41598-022-24109-5
- B. Boeckx, G. Maes, J. Phys. Chem. B 2012, 116, 12441–12449.
 DOI:10.1021/jp306916e
- 11. R. Breslow, Z. L. Cheng, *Proc. Natl. Acad. Sci.* **2010**, *13*, 5723–5725. **DOI:**10.1073/pnas.1001639107
- 12. M. J. Barker, J. Trevisan, P. Bassan, R. Bhargava, H. J. Butler, K. M. Dorling, P. R. Fielden, S. W. Fogarty, N. J. Fullwood, K. A. Heys, C. Hughes, P. Lasch, P. L. Martin-Hirsch, B. Obinaju, G. D. Sockalingum, J. Sulé-Suso, R. J. Strong, M. J. Walsh, B. R. Wood, P. Gardner, F. L. Martin, *Nat. Prot.* 2014, 9, 1771–1791. DOI:10.1038/nprot.2014.110
- 13. Y. Gonda, A. Matsuda, K. Adachi, C. Ishii, M. Suzuki, A. Osaki, M. Mita, N. Nishizaki, Y. Ohtomo, T. Shimizu, M. Yasui, K. Hamase, J. Sasabe, *Proc. Natl. Acad. Sci.* 2023, 120, e2300817120. DOI:10.1073/pnas.2300817120
- P. R. Tulip, S. J. Clark. *Phys. Rev. B* **2005**, *71*, 195117.
 DOI:10.1103/PhysRevB.71.195117
- 15. N. A. Bowden, J. P. M. Sanders, M. E. Bruins, *J. Chem. Eng. Data* **2018**, *63*, 488–497. **DOI:**10.1021/acs.jced.7b00486
- S. Lakhera, M. Rana, K. Devlal, Opt. Quant. Elect. 2022, 54, 4118–4. DOI:10.1007/s11082-022-04118-4
- M. Aliyeva, P. Brandão, J. R. B. Gomes, J. A.P. Coutinho, O. Ferreira, S. P. Pinho, *Ind. Eng. Chem. Res.* 2022, *61*, 5620–5631.
 DOI:10.1021/acs.iecr.1c04562

- X. Liu, M. Wu, C. Li, P. Yu, S. Feng, Y. Li, Q. Zhang, *Molecules* 2022, 27, 2407. DOI:10.3390/molecules27154870
- M. Barria-Urrenda, A. Ruiz-Fernandez, C. Gonzalez, C. Oostenbrink, J. A. Garate, *J. Chem. Inf. Model.* **2023**, *63*, 6642–6654. **DOI**:10.1021/acs.jcim.3c00418
- N. Fujii, Orig. Life Evol. 2002, 32, 103–127
 DOI:10.1023/A:1016031014871
- 21. F. Cava, H. Lam, M. A. de-Pedro, M. K. Waldor, *Cell. Mol. Life Sci.* **2011**, *68*, 817–831. **DOI:**10.1007/s00018-010-0571-8
- J. J. A.J. Bastings, H. M. van Eijk, S. W. Olde Damink, S. S. Rensen, *Nutrients* 2019, *11*, 2205–2222.
 DOI:10.3390/nu11092205
- R. Dalangin, A. Kim, R. E. Campbell, *Int. J. Mol. Sci.* 2020, *21*, 6197–6232. DOI:10.3390/ijms21176197
- 24. A. Hallen, J. F. Jamie, A. J. L. Cooper, *Amino Acids* **2013**, *45*, 1249–1272. **DOI**:10.1007/s00726-013-1590-1
- H. Ohide, Y. Miyoshi, R. Maruyama, K. Hamase, R. Konno, *J. Chromat. B* 2011, 879, 3162–3168.
 DOI:10.1016/j.jchromb.2011.06.028
- J. M. Seckler, S. J. Lewis, J. Molec. Sci. 2020, 21, 7325–7343.
 DOI:10.3390/ijms21197325
- 27. M. Hu, F. He, E. W. Thompson, K. Ostrikov, X. Dai, *Cancers* **2022**, *14*, 346–363. **DOI**:10.3390/cancers14020346
- 28. M. Poline, O. Rebrov, M. Larsson, V. Zhaunerchyk. *Chirality* **2020**, 32, 359–369. **DOI**:10.1002/chir.23165
- A. Aliashkevich, L. Alvarez, F. Cava, Front. Microbiol. 2018, 9,
 DOI:10.3389/fmicb.2018.00683
- Q. Xu, H. Deng, X. Li, Z. X. Quan, Front. Chem. 2021, 9, 650569
- 31. B. Boeckx, G. Maes; *J. Phys. Chem. B* **2012**, *116*, 12441–12449 **DOI:**10.1021/jp306916e
- L. Stagi, M. Sini, D. Carboni, R. Anedda, G. Siligardi, T. M. Gianga, R. Hussain, P. Innocenzi, *Sci. Rep.* 2022, *12*, 19719.
 DOI:10.1038/s41598-022-24109-5
- 33. P. Kratzer, J. Neugebauer, *Front. Chem.* **2019**, *7*, 106. **DOI:**10.3389/fchem.2019.00106
- J. L. Cabellos, F. Ortiz-Chi, A. Ramírez, G. Merino, 2013, Bilatu 1.0, Mérida, Cinvestav.
- 35. M. Saunders, *J. Comput. Chem.* **2004**, *25*, 621–626. **DOI:**10.1002/jcc.10407
- 36. F. Neese, The ORCA program system, *Wiley Interdiscip. Rev.:* Comput. Mol. Sci. **2012**, 2, 73–78. **DOI**:10.1002/wcms.81

- C. Adamo, V. Barone, J. Chem. Phys. 1999, 110, 6158–6170.
 DOI:10.1063/1.478522
- 38. F. Weigend, *Phys. Chem. Chem. Phys.* **2006**, *8*, 1057–1065. **DOI:**10.1039/b515623h
- 39. S. Grimme, J. Antony, S. Ehrlich, H. A. Krieg, *J. Chem. Phys.* **2010**, *132*, 154104. **DOI:**10.1063/1.3382344
- 40. S. Schlund, R. Müller, C. Graβmann, B. Engels, *J. Comput. Chem.* **2008**, *29*, 407–415. **DOI:**10.1002/jcc.20798
- C. E. Buelna-García, E. Robles-Chaparro, T. Parra-Arellano, J. M. Quiroz-Castillo, T. del-Castillo-Castro, G. Martínez-Guajardo, C. Castillo-Quevedo, A. de-Leon-Flores, G. Anzueto-Sánchez, M. F. Martin-del-Campo-Solis, A. M. Mendoza-Wilson, A. Vásquez-Espinal, J. L. Cabellos, *Molecules* 2021, 26, 3953–3976. DOI:10.3390/molecules26133953
- C. E. Buelna-García, J. L. Cabellos, J. M. Quiroz-Castillo, G. Martínez-Guajardo, C. Castillo-Quevedo, A. de Leon-Flores, G. Anzueto-Sánchez, M. F. Martín-del-Campo-Solís, *Materials* 2021, 14, 112–138. DOI:10.3390/ma14010112
- 43. M. F. Kemmere, T. F. Keurentjes, in: S. P. Nunes, K. V. Peinemann (Ed.): Membrane Technology in the Chemical Industry, Wiley-VCH, Weinheim, Germany, 2008, pp. 229–255.
- 44. C. Riplinger, B. Sandhoefer, A. Hansen, F. Neese, *J. Chem. Phys.* **2013**, *139*, 134101. **DOI:**10.1063/1.4821834
- J. Tomasi, B. Mennucci, R. Cammi, Chem. Rev. 2005, 105, 2999–3094. DOI:10.1021/cr9904009
- R. K. Pathria, P. D. Beale, 2011. Statistical Mechanics (3rd ed.). Elsevier. Chapter 4.
- L. E. Reichl, 2016. A Modern Course in Statistical Physics. Wiley-VCH. DOI:10.1002/9783527690497
- 48. J. R. Lakowicz **2006**. Principles of Fluorescence Spectroscopy (3rd ed.). Springer. **DOI:**10.1007/978-0-387-46312-4
- 49. A. de Leon, J. L. Cabellos, C. Castillo-Quevedo, M. F. Martín-del-Campo-Solís, G. Martínez-Guajardo, *Acta Chim. Slov.* **2023**, *70*, 642–650. **DOI:**10.17344/acsi.2023.8435
- 50. C. E. Buelna-García, C. Castillo-Quevedo, J. M. Quiroz-Castillo, E. Paredes-Sotelo, M. Cortez-Valadez, M. F. Martin-del-Campo-Solis, T. López-Luke, M. Utrilla-Vázquez, A. M. Mendoza-Wilson, P. L. Rodríguez-Kessler, A. Vazquez-Espinal, S. Pan, A. de Leon, J. R. Mis-May, A. R. Rodríguez-Domínguez, G. Martínez-Guajardo, J. L. Cabellos, Front. Chem. 2022, 10, 841964. DOI:10.3389/fchem.2022.841964

Povzetek

Ta študija raziskuje konformacijske in termokemijske lastnosti lizina z uporabo kvantno kemijskih računskih metod na ravni teorije PBE0-GD3/Def2-TZVP za optimizacijo geometrije in CCSD(T)/Def2-TZVP za izračun termičnih korekcij potencialne energije. Lizin tvori psevdociklične konformacije, stabilizirane z vodikovimi vezmi med amino in karboksilnimi skupinami. Identificirali smo 36 konformerov, enakomerno razdeljenih med L- in D-lizin, z majhnimi razlikami v energiji med strukturami. Ko je psevdociklična konformacija prekinjena, to močno vpliva na energijo. Konformacije lizina so izjemno občutljive na temperaturo. Ugotovitve poudarjajo temperaturno občutljivost lizina in njegov potencial za raznolike uporabe. Njegova strukturna prilagodljivost v območju od 0 do 1800 K nakazuje na potencialno uporabo v materialih, kot so temperaturno odzivne tanke plasti polprevodnikov, premazi, senzorji, kataliza prek nastavljivih aktivnih mest ter v biomedicini za dostavo zdravil ali stabilizacijo proteinov. Vpogledi, ki jih ponuja ta študija, poudarjajo vsestranskost lizina kot biomolekule in njegovo možno uporabo za tehnološke inovacije na različnih področjih.



Except when otherwise noted, articles in this journal are published under the terms and conditions of the Creative Commons Attribution 4.0 International License